

Light storage in coherently excited nitrogen ions

Jinping Yao^{1,#}, LuoJia Wang^{2,#}, Jinming Chen^{1,3,4}, Yuexin Wan^{1,3}, Zhihao Zhang^{1,3,4},
Fangbo Zhang^{1,3}, Lingling Qiao¹, Shupeng Yu^{1,3}, Botao Fu^{1,3,4}, Zengxiu Zhao⁵,
Chengyin Wu⁶, Vladislav V. Yakovlev⁷, Luqi Yuan^{2,*}, Xianfeng Chen^{2,8,9,*}, and Ya
Cheng^{1,9,10,*}

¹*State Key Laboratory of High Field Laser Physics and CAS Center for Excellence in Ultra-intense Laser Science, Shanghai Institute of Optics and Fine Mechanics (SIOM), Chinese Academy of Sciences (CAS), Shanghai 201800, China*

²*State Key Laboratory of Advanced Optical Communication Systems and Networks, School of Physics and Astronomy, Shanghai Jiao Tong University, Shanghai 200240, China*

³*University of Chinese Academy of Sciences, Beijing 100049, China*

⁴*School of Physical Science and Technology, ShanghaiTech University, Shanghai 200031, China*

⁵*Department of Physics, National University of Defense Technology, Changsha 410073, China*

⁶*State Key Laboratory for Mesoscopic Physics, School of Physics, Peking University, Beijing 100871, China*

⁷*Texas A&M University, College Station, TX 77843, USA*

⁸*Jinan Institute of Quantum Technology, Jinan 250101, China*

⁹*Collaborative Innovation Center of Light Manipulations and Applications, Shandong Normal University, Jinan 250358, China*

¹⁰*Collaborative Innovation Center of Extreme Optics, Shanxi University, Taiyuan, Shanxi 030006, China*

[#]These authors contributed equally to this work.

*Corresponding authors: yuanluqi@sjtu.edu.cn; xfchen@sjtu.edu.cn; ya.cheng@siom.ac.cn

Abstract:

Quantum memory is an essential part of quantum computer and quantum information storage. Alkali metal vapors are traditionally used as a medium due to convenient near-infrared excitation, strong dipole transitions and long-lived coherence. Here, we proposed and experimentally demonstrated the optical storage in coherently excited molecular nitrogen ion (N_2^+) which is produced using a strong 800 nm femtosecond laser pulse. Such optical storage facilitated by quantum coherence keeps releasing weak coherent emission for tens of picoseconds and can be read-out by a time-delayed femtosecond pulse centered at 1580 nm via two-photon resonant absorption, resulting in a strong radiation at 329.3 nm. We reveal a pivotal role of the $B^2\Sigma_u^+(v=4)$ excited state to transmit even extremely weak stored light in such system. This new finding unveils the nature of the coherent quantum control in N_2^+ for the potential platform for quantum memory storage in the remote atmosphere, and facilitates further exploration of fundamental interactions in the quantum optical platform with strong-field ionized molecules.

Quantum coherence plays a central role in modern developments of quantum optics [1-3], which is of fundamental importance for understanding and predicting many initially counter-intuitive physical phenomena such as electromagnetically induced transparency [4-7], lasing without inversion [8-10], and mirrorless laser-like emission [11-13]. The optical quantum memory, or the light storage with quantum coherence, is of essential for achieving optical information storage in quantum communications [14-18], yet, many existing proposals require alkali metal vapor medium, which possibly hinders the broad range of applications.

For several decades, alkali metal atoms have been serving as a backbone of quantum optical platforms [19-21] due to a number of unique properties such as sufficiently long coherence time, the lack of inter-vibrational relaxation, and easy access to laser wavelengths capable of the resonant excitation. Alkali metal dimers, which can be created through heating atoms at a high temperature, are another promising candidate for coherent quantum control [22-25]. Nevertheless, it would be of great importance to explore alternative solutions involving more abundant elements and molecules which are also less chemically reactant and safe to use. In particular, molecular nitrogen ions (N_2^+), which can easily be produced from atmospheric nitrogen using high-intensity femtosecond pulses, emerge as the intriguing model system for exploring quantum coherence effects from abundant energy levels that exhibit rich electron and molecular dynamics [26-32]. In such a system, the energy diagram is significantly different from that of an atom, i.e., energy differences between lower electronic states of molecular ions are located in near-ultraviolet, visible and near-infrared spectral regions, making it easy to efficiently manipulate the quantum coherence between multiple states by using commonly available lasers. Electronic, vibrational, and rotational coherences are created in molecular ions when electron instantaneously escapes from nucleus in a strong laser field [27]. However, the quantum coherence in strong-field-ionized molecular ions remains largely unexplored, opening the venue for achieving optical quantum memory and for exploring coherent quantum control in excited nitrogen ions.

In this Letter, we demonstrate the optical storage in N_2^+ both theoretically and experimentally. The proposed idea of achieving the light storage using N_2^+ quantum optical platform is briefly illustrated in Fig. 1. Three electronic states of N_2^+ , i.e., $X^2\Sigma_g^+$, $A^2\Pi_u$ and $B^2\Sigma_u^+$ (abbreviated as X , A and B), are considered to construct a three-level system as shown in Fig. 1(b). An intense laser at 800 nm is used to ionize molecular N_2 into N_2^+ and to pump N_2^+ into the excited A state. The same laser also generates the quantum coherence between X and A states, which keeps re-emitting photons near 800 nm for the timescale of picoseconds. Another laser at 1580 nm is injected after the picosecond delay to readout re-emitted photons. The delayed 1580 nm photons interact with stored photons to promote the two-photon resonance, which, in its turn, leads to an experimentally observed strong emission at 329.3 nm. In the same time, the population on $B(v=4)$ level significantly amplifies the contribution of the coherently-stored light, resulting in strong 329.3 nm emission, which persists even tens of picosecond after the initial excitation by the 800 nm laser. This report exhibits important coherent quantum control of light in N_2^+ , which points to potential applications of quantum computations and quantum simulations with ions, and also an exciting perspective for remote atmospheric coherent light storage at room temperature.

As shown in Fig. 1, a femtosecond laser at 800 nm excites the quantum coherence ρ_{AX} . Under the perturbation theory in the weak excitation limit, we have $\rho_{AX}(t) \propto iE_1^p \delta t [\rho_{XX}(0) - \rho_{AA}(0)] e^{-\Gamma t}$, where E_1^p is the peak amplitude of the 800 nm laser field, δt is the full width at half maximum of the laser field, Γ is the dephasing rate, and $\rho_{ii}(0)$ is the initial population at the level i . Such coherence keeps emitting photons near 800 nm with the coherence time up-to picoseconds, with its intensity being approximately described as $I_S(t) \propto |E_1^p \delta t [\rho_{XX}(0) - \rho_{AA}(0)]|^2 e^{-2\Gamma t}$. Another laser at 1580 nm with the peak amplitude E_2^p and the same pulse duration is applied at a delay τ , and is used to read-out the stored photon, which triggers a two-photon absorption (TPA) between levels A and B . The TPA rate can be estimated as $|E_1^p E_2^p \delta t^2|^2 [\rho_{XX}(0) - \rho_{AA}(0)]^2 [\rho_{BB}(0) - \rho_{AA}(0)]^2 e^{-2\Gamma \tau}$. The ultraviolet (UV) radiation from level B to X is then generated and detected. Since the initial excitation

(at 800 nm) can be stored in the coherence ρ_{AX} in N_2^+ for a relatively long time $\sim 1/\Gamma$ after the 800 nm laser is gone, such stored light can be read-out by a delayed 1580 nm laser through the TPA process within the time window defined by $\sim 1/\Gamma$. In the following, we will first demonstrate the experimental results to validate our hypothesis of light storage and then support the experimental data with more accurate numerical simulations to further explore the effect.

With the basic concept of our proposal in mind, we designed our experiment in the nitrogen gas. A commercial Ti:sapphire laser (Legend Elite-Duo, Coherent, Inc.) was used to pump an optical parametric amplifier (OPA), which delivered femtosecond laser pulses tunable from 1200 nm to 2400 nm. The remaining fundamental radiation centered at 800 nm was used as a pump beam to promote N_2^+ generation. The polarization directions of two laser beams were parallel to each other, and their relative delay was controlled by a motorized translation stage. Two beams were combined using a dichroic mirror and collinearly focused into 5-mbar nitrogen gas using a plano-convex lens ($f = 20$ cm). The peak intensity at the focus was $\sim 2 \times 10^{14}$ W/cm² for the 800-nm, 40-fs laser pulse and $\sim 1 \times 10^{13}$ W/cm² for the 1580-nm, 60-fs laser pulse, where two laser fields were assumed to have Gaussian shapes in both space and time. The UV radiation exiting from the gas chamber was collected and focused onto a slit of a spectrometer (Shamrock 303i, Andor) for spectral analysis. A set of appropriate filters were placed before the spectrometer to block the residual laser radiation.

Figure 2(a) shows the energy diagram for the UV generation through the resonant interaction of two laser fields with N_2^+ . The 800 nm laser (ω_1) was used for the ionization of N_2 molecules and photo-excitation of N_2^+ from X to A state. Afterwards, N_2^+ ions were excited to B state by absorbing a photon near 800 nm and a photon near 1580 nm (ω_2). The cascaded resonant excitation gave rise to a strong radiation at 329.3 nm. Figure 2(b) shows typical spectra of UV radiations induced by 800 nm and 1580 nm lasers for different time delays: $\tau = 0$ and $\tau = 1$ ps. At $\tau = 0$, a strong radiation at 329.3 nm wavelength was superimposed on a broad spectrum produced by the non-resonant four-wave mixing (FWM). The narrow-bandwidth radiation at 329.3 nm is ascribed to P branch of $B(v=4) \rightarrow X(v=2)$, whereas the side lobe near 328 nm is ascribed to R branch of the same electronic transition. They were generated by resonant FWM

of two lasers in N_2^+ . We observed another narrow-bandwidth radiation at 330.8 nm wavelength, which corresponds to $B(v=2) \rightarrow X(v=0)$ transition. Although the broadband FWM spectrum was also able to cover this transition, the 330.8 nm signal was much weaker than the 329.3 nm radiation. At $\tau = 1$ ps, both the non-resonant FWM signal and 330.8 nm radiation disappeared due to the temporal separation of two pulses. Nevertheless, the 329.3 nm radiation measured at two delays remained almost unchanged.

Figure 2(c) compares the evolution of the non-resonant FWM at 321.0 nm and the resonant FWM at 329.3 nm with the time delay. Unlike the non-resonant FWM which required the temporal overlap of two laser fields, the 329.3 nm signal reached its maximum around the zero delay and almost remained unchanged over the next several picoseconds except for some oscillations caused by molecular rotations. When the dynamics was measured over a longer timescale, as illustrated in Fig. 2(d), the 329.3 nm signal exhibited an exponential decay with a time constant of ~ 26 ps. Generation of the 329.3 nm radiation after the temporal separation of two laser pulses indicates that TPA from $A(v=4)$ to $B(v=4)$ was triggered by the stored light and the delayed-injected 1580 nm laser.

We further studied the UV radiation driven by the 800 nm laser field and the delay-injected laser with other wavelengths. When the laser wavelength was tuned to 1910 nm, two-photon resonance from $A(v=4)$ to $B(v=4)$ was no longer satisfied. In this case, the narrow-bandwidth radiation at 329.3 nm was submerged by the non-resonant FWM signal [see inset of Fig. 3(a)]. Similar to other spectral components of FWM, the radiation at 329.3 nm was only observed within the temporal overlap of two laser fields, as illustrated in Fig. 3(a). The comparison between Fig. 2(c) and Fig. 3(a) clearly demonstrates that the cascaded resonant condition in the three-level N_2^+ system must be fulfilled to generate the strong 329.3 nm radiation after the temporal separation of two laser fields, which agrees with our predication in Fig. 1. When the wavelength of the delayed laser field was tuned to 2070 nm, we could realize one-photon resonant excitation from $X(v=0)$ to $A(v=2)$ and two-photon resonant excitation from $A(v=2)$ to $B(v=2)$ [see Fig. 2(a)]. Although the cascaded resonant condition similar to the 329.3 nm radiation was fulfilled, the 330.8 nm radiation was only observed around zero delay,

as shown in Fig. 3(b). This difference for different transitions was beyond our expectation, and hence detailed simulation was necessary to gain a better fundamental understanding.

We performed numerical simulations using Maxwell-Bloch equations. We considered a one-dimensional pencil-like medium with N_2^+ modeled by a three-level diagram (i.e., $X(v=2)$, $A(v=4)$, $B(v=4)$) shown in Fig. 2(a). The two-photon excitation of the $A \leftrightarrow B$ transition was treated as two excitation processes via two dipole-allowed transitions with a detuned intermediate level I [33]. Using the rotating-wave approximation, the Hamiltonian in the interaction picture reads [1]

$$H = \hbar\Delta|I\rangle\langle I| + (-\wp_{AX}E_1|A\rangle\langle X| - \wp_{IA}E_1|I\rangle\langle A| - \wp_{BI}E_2|B\rangle\langle I| - \wp_{BX}E_s|B\rangle\langle X| + \text{H.c.}), \quad (1)$$

where \wp_{ij} is the dipole moment between the $i \leftrightarrow j$ transition, $E_{1(2)}$ is the slowly varying envelope amplitude of the 800 (1580) nm electric field, and $\Delta = \omega_{IA} - \omega_1$ is the detuning between $A \leftrightarrow I$ transition and the 800 nm laser field. Assuming Δ is much larger than any decoherence rate and thus ρ_{IX} is negligible, one can use steady-state values $\rho_{IA} = [\wp_{IA}E_1(\rho_{AA} - \rho_{II}) + (\wp_{BI}E_2)^*\rho_{BA}]/(\hbar\Delta)$ and $\rho_{BI} = [\wp_{BI}E_2(\rho_{BB} - \rho_{II}) + (\wp_{IA}E_1)^*\rho_{BA}]/(\hbar\Delta)$. Hence, the two-photon excitation can be described effectively in the density-matrix equations [33]:

$$\dot{\rho}_{AX} = -\Gamma_{AX}\rho_{AX} + i\frac{\wp_{AX}E_1}{\hbar}(\rho_{XX} - \rho_{AA}) - i\frac{\wp_{BX}E_s}{\hbar}\rho_{AB}, \quad (2)$$

$$\begin{aligned} \dot{\rho}_{BA} = & \left(-\Gamma_{BA} + i\frac{|\wp_{BI}E_2|^2 - |\wp_{IA}E_1|^2}{\hbar^2\Delta} \right) \rho_{BA} \\ & + i\frac{\wp_{BI}E_2\wp_{IA}E_1}{\hbar^2\Delta}(\rho_{AA} - \rho_{BB}) - i\frac{(\wp_{AX}E_1)^*}{\hbar}\rho_{BX} + i\frac{\wp_{BX}E_s}{\hbar}\rho_{XA}, \end{aligned} \quad (3)$$

$$\dot{\rho}_{BX} = -\Gamma_{BX}\rho_{BX} + i\frac{\wp_{BX}E_s}{\hbar}(\rho_{XX} - \rho_{BB}) - i\frac{\wp_{AX}E_1}{\hbar}\rho_{BA}, \quad (4)$$

$$\dot{\rho}_{BB} = -\gamma_B\rho_{BB} + \left(i\frac{\wp_{BI}E_2\wp_{IA}E_1}{\hbar^2\Delta}\rho_{AB} + i\frac{\wp_{BX}E_s}{\hbar}\rho_{XB} + \text{H.c.} \right), \quad (5)$$

$$\dot{\rho}_{AA} = -\gamma_A\rho_{AA} + \left(-i\frac{\wp_{BI}E_2\wp_{IA}E_1}{\hbar^2\Delta}\rho_{AB} + i\frac{\wp_{AX}E_1}{\hbar}\rho_{XA} + \text{H.c.} \right), \quad (6)$$

$$\rho_{XX} + \rho_{AA} + \rho_{BB} = 1, \quad (7)$$

where dephasing rates are $\Gamma_{AX} = \frac{1}{2}\gamma_A + \gamma_{col}$, $\Gamma_{BA} = \frac{1}{2}(\gamma_A + \gamma_B) + \gamma_{col}$, $\Gamma_{BX} = \frac{1}{2}\gamma_B +$

γ_{col} , with γ_{col} being the collisional dephasing rate, and $\gamma_{A(B)}$ is the spontaneous decay rate from level $A(B)$. The Maxwell equations for field amplitudes read

$$\frac{\partial E_s}{\partial z} + \frac{1}{c} \frac{\partial E_s}{\partial t} = i\eta_{BX}\rho_{BX}, \quad (8)$$

$$\frac{\partial E_1}{\partial z} + \frac{1}{c} \frac{\partial E_1}{\partial t} = i\eta_{AX}\rho_{AX}, \quad (9)$$

where $\eta_{iX} = 3\hbar n_a \lambda_{iX}^2 \gamma_i / (8\pi \wp_{iX})$, λ_{iX} is the transition wavelength, and n_a is the N_2^+ density. We simulate the FWM signal E_s as well as the E_1 field followed by a delayed E_2 laser field by solving the Maxwell-Bloch equations (2)-(9). In simulations, we set parameters: the medium length as 0.15 mm, $\gamma \sim 0.01 \text{ ns}^{-1}$, $\gamma_{col} \sim 1 \text{ ns}^{-1}$, $\wp \sim 10^{-3} \text{ C} \cdot \text{m}$, $\Delta \sim 10^{15} \text{ rad/s}$, and $n_a = 4 \times 10^{16} \text{ cm}^{-3}$. Peak amplitudes of two original lasers are set as $E_1^p \sim 3 \times 10^{10} \text{ V/m}$ and $E_2^p \sim 0.7 \times 10^{10} \text{ V/m}$, respectively. Both two laser pulses have a Gaussian intensity envelope with the pulse duration of 50 fs.

We plot numerical results for evolutions of the 800 nm laser and ρ_{BA} for the cases of $\tau = 0$ and $\tau = 1 \text{ ps}$ in Fig. 4. Results for different initial population $\rho_{BB}(0)$ on level B are considered. After original 800 nm laser passes through the medium, the calculated laser field shows a long tail with oscillations. The tail is 7~8 orders of magnitude weaker than the main peak, and the intensity ratio of the main peak and the tail is almost independent of $\rho_{BB}(0)$. The tail means that ρ_{BA} is generated and continuously releases weak emission around 800 nm, which is consistent with the theory that light storage happens and photons are stored and re-emitted. Such the weak light stored in the medium can then be read-out when the 1580 nm laser field is injected with the time delay. For the case of $\tau = 1 \text{ ps}$, the coherence ρ_{BA} between levels A and B arises due to the two-photon excitation process, and reaches a larger amplitude as $\rho_{BB}(0)$ increases [see Fig. 4(c)]. Although ρ_{BA} is much smaller at $\tau = 1 \text{ ps}$ than that at $\tau = 0$, it is still possible to generate 329.3 nm radiation through the resonant FWM provided the stored photon near 800 nm keeps pumping ions.

To give a straightforward comparison with experimental results, we plotted calculated spectra of signal fields and integrals of signal intensities versus delay for different $\rho_{BB}(0)$. Signal field spectra for simultaneous pumping from two fields in Fig. 5(a) show a Fano line shape, while the signal field at $\tau = 1$ ps evolves in a large time scale resulting in a narrow spectral line in Fig. 5(b). In contrast to the case of $\tau = 0$, the 329.3 nm signal at $\tau = 1$ ps grows dramatically as $\rho_{BB}(0)$ increases. This dependence is also shown in curves of the total signal versus delay. As shown in Fig. 5(c), a larger $\rho_{BB}(0)$ results in a smaller decrease of the intensity versus the delay. For the case of $\rho_{BB}(0) = 0$, the 329.3 nm signal at $\tau = 1$ ps is about 10 orders of magnitude weaker than that at $\tau = 0$. Such a weak signal is impossible to be measured experimentally. Furthermore, after the initially quick drop, the decay rate of the signal becomes smaller, which is consistent with the experimental result in Fig. 2(c). The simulation results show that B -state population is of vital importance for reading-out the stored photon. The high population on $B(v=4)$ level makes the read-out process be significantly improved, allowing us to experimentally observe the stored photons through the 329.3 nm radiation.

Actually, the $B(v=4)$ level can be efficiently populated through three-photon near-resonant excitation shown in Fig. 2(a), which has been demonstrated in previous simulations [28,30]. To confirm this fact experimentally, we injected a femtosecond seed pulse around 330 nm after the 800 nm laser. Although the seed pulse can cover all transitions $B(v=2,3,4) \rightarrow X(v=0,1,2)$ with $\Delta v = 2$, it is only amplified at 329.3 nm, as shown in Fig. 3(c), indicating that the $B(v=4)$ level has a higher population than the $X(v=2)$ level. For the three-level system composed of $X(v=2)$, $A(v=4)$ and $B(v=4)$, the high population probability on $B(v=4)$ level makes the 329.3 nm radiation easily be obtained with two temporal separated laser fields. In comparison, the absorption at 330.8 nm means that more ions are populated on the $X(v=0)$ level. Low population on the $B(v=2)$ level makes the 330.8 nm radiation cannot be efficiently generated after the separation of two lasers, which is consistent with the experimental result in Fig. 3(b). Our numerical simulation results convincingly prove the proposed light storage and

show excellent qualitative agreement with experimental measurements. Further improvement in simulations is possible if we include more realistic beam profiles of lasers, inhomogeneous density distribution of N_2^+ , and the dynamic ionization process, which, however, increases the numerical difficulty.

To conclude, we have demonstrated for the first time the light storage and optical readout in the quantum optical platform made out of nitrogen ions. Photons near 800 nm are stored in the quantum coherence in N_2^+ , which are then read-out by applying a delayed 1580 nm laser to induce the UV radiation. Moreover, large population on the $B(v=4)$ level is produced through the three-photon excitation, which largely enhances the read-out signal. Our work reveals the light storage in ionic nitrogen, which triggers a broad interest for potential applications involving those ions including remote sensing [27], quantum computation [34], and quantum simulations [35]. Our pioneering experiment performed in molecular nitrogen with tunnel ionization also opens an important route towards future potential implementation optical quantum memory in remote atmospheric regime.

This work is supported by National Natural Science Foundation of China (11822410, 12034013, 11734009, 11974245); National Key R&D Program of China (2017YFA0303701); Shanghai Municipal Science and Technology Major Project (2019SHZDZX01); Program of Shanghai Academic Research Leader (20XD1424200); Natural Science Foundation of Shanghai (19ZR1475700); Strategic Priority Research Program of Chinese Academy of Sciences (XDB16030300); Key Research Program of Frontier Sciences of Chinese Academy of Sciences (QYZDJ-SSW-SLH010); Youth Innovation Promotion Association of CAS (2018284); NSF (ECCS-1509268, CMMI-1826078) and AFOSR (FA9550-20-1-0366, FA9550-20-1-0367).

References:

- [1] M. O. Scully and M. S. Zubairy, *Quantum Optics* (Cambridge University, 1997).
- [2] P. Kok, B. W. Lovett, *Introduction to Optical Quantum Information Processing* (Cambridge University Press, Cambridge 2010).
- [3] M. D. Lukin, Rev. Mod. Phys. **75**, 457 (2003).
- [4] M. Fleischhauer, A. Imamoglu, and J. P. Marangos, Rev. Mod. Phys. **77**, 633 (2005).
- [5] S. E. Harris, J. E. Field, and A. Imamoglu, Phys. Rev. Lett. **64**, 1107 (1990).
- [6] K. J. Boller, A. Imamoglu, and S. E. Harris, Phys. Rev. Lett. **66**, 2593 (1991).
- [7] R. Röhlsberger, H.-C. Wille, K. Schlage, and B. Sahoo, Nature **482**, 199 (2012).
- [8] O. A. Kocharovskaya and Ya. I. Khanin, J. Exp. Theor. Phys. **48**, 630 (1988).
- [9] S. E. Harris, Phys. Rev. Lett. **62**, 1033 (1989).
- [10] M. O. Scully, S.-Y. Zhu, and A. Gavrielides, Phys. Rev. Lett. **62**, 2813 (1989).
- [11] A. E. Siegman, *Lasers* (University Science Books, Sausalito, CA).
- [12] A. Dogariu, J. B. Michael, M. O. Scully, and R. B. Miles, Science **331**, 442 (2011).
- [13] A. J. Traverso, R. Sanchez-Gonzalez, L. Yuan, K. Wang, D. V. Voronine, A. M. Zheltikov, Y. Rostovtsev, V. A. Sautenkov, A. V. Sokolov, S. W. North, and M. O. Scully, Proc. Natl. Acad. Sci. USA **109**, 15185 (2012).
- [14] D.-W. Wang and M. O. Scully, Phys. Rev. Lett. **113**, 083601 (2014).
- [15] O. Katz and O. Firstenberg, Nat. Commun. **9**, 2074 (2018).
- [16] A. Zhang, L. Wang, X. Chen, V. V. Yakovlev, and L. Yuan, Commun. Phys. **2**, 157 (2019).
- [17] Z. Wang, H. Li, W. Feng, X. Song, C. Song, W. Liu, Q. Guo, X. Zhang, H. Dong, D. Zheng, H. Wang, and D.-W. Wang, Phys. Rev. Lett. **124**, 013601 (2020).
- [18] W. S. Leong, M. Xin, C. Huang, Z. Chen, and S.-Y. Lan, Phys. Rev. Res. **2**, 033320 (2020).
- [19] A. D. Cronin, J. Schmiedmayer, and D. E. Pritchard, Rev. Mod. Phys. **81**, 1051 (2009).
- [20] K. Hammerer, A. S. Sørensen, and E. S. Polzik, Rev. Mod. Phys. **82**, 1041

(2010).

- [21] M. S. Safronova, D. Budker, D. DeMille, D. F. J. Kimball, A. Derevianko, and C. W. Clark, *Rev. Mod. Phys.* **90**, 025008 (2018).
- [22] V. V. Yakovlev, C. J. Bardeen, J. Che, J. Cao, and K. R. Wilson, *J. Chem. Phys.* **108**, 2309 (1998).
- [23] T. Brixner, G. Krampert, T. Pfeifer, R. Selle, G. Gerber, M. Wollenhaupt, O. Graefe, C. Horn, D. Liese, and T. Baumert, *Phys. Rev. Lett.* **92**, 208301 (2004).
- [24] L. Yuan, G. O. Ariunbold, R. K. Murawski, D. Pestov, X. Wang, A. K. Patnaik, V. A. Sautenkov, A. V. Sokolov, Y. V. Rostovtsev, and M. O. Scully, *Phys. Rev. A* **81**, 053405 (2010).
- [25] L. Rybak, S. Amaran, L. Levin, M. Tomza, R. Moszynski, R. Kosloff, C. P. Koch, and Z. Amitay, *Phys. Rev. Lett.* **107**, 273001 (2011).
- [26] J. Yao, B. Zeng, H. Xu, G. Li, W. Chu, J. Ni, H. Zhang, S. L. Chin, Y. Cheng, and Z. Xu, *Phys. Rev. A* **84**, 051802(R) (2011).
- [27] L. Yuan, Y. Liu, J. Yao, and Y. Cheng, *Adv. Quantum Technol.* **2**, 1900080 (2019).
- [28] J. Yao, S. Jiang, W. Chu, B. Zeng, C. Wu, R. Lu, Z. Li, H. Xie, G. Li, C. Yu, Z. Wang, H. Jiang, Q. Gong, and Y. Cheng, *Phys. Rev. Lett.* **116**, 143007 (2016).
- [29] H. Li, M. Hou, H. Zang, Y. Fu, E. Lötstedt, T. Ando, A. Iwasaki, K. Yamanouchi, and H. Xu, *Phys. Rev. Lett.* **122**, 013202 (2019).
- [30] Q. Zhang, H. Xie, G. Li, X. Wang, H. Lei, J. Zhao, Z. Chen, J. Yao, Y. Cheng, and Z. Zhao, *Commun. Phys.* **3**, 50 (2020).
- [31] M. Richter, M. Lytova, F. Morales, S. Haessler, O. Smirnova, M. Spanner, and M. Ivanov, *Optica* **7**, 586 (2020).
- [32] W. Zheng, Z. Miao, L. Zhang, Y. Wang, C. Dai, A. Zhang, H. Jiang, Q. Gong, and C. Wu, *J. Phys. Chem. Lett.* **10**, 6598 (2019).
- [33] L. Yuan, B. H. Hokr, A. J. Traverso, D. V. Voronine, Y. Rostovtsev, A. V. Sokolov, and M. O. Scully, *Phys. Rev. A* **87**, 023826 (2013).
- [34] H. Haffner, C. F. Roos, and R. Blatt, *Phys. Rep.* **469**, 155 (2008).
- [35] I. M. Georgescu, S. Ashhab, and F. Nori, *Rev. Mod. Phys.* **86**, 153 (2014).

Captions of figures:

Fig. 1 (a) Schematic for achieving the light storage with N_2^+ ions and (b) the corresponding energy-level schemes. The 800 nm laser excites the electronic coherence between levels X and A , which keeps emitting photons near 800 nm. A delayed 1580 nm laser is used to readout the re-emitted photon via TPA, which then generates the UV radiation.

Fig. 2 (a) Energy diagram of the resonant excitation in N_2^+ for generating UV radiations at 329.3 nm and 330.8 nm. (b) Spectra of UV radiations induced by the 800 nm and 1580 nm lasers in the cases of $\tau = 0$ and $\tau = 1$ ps. (c) The evolution of resonant FWM at 329.3 nm and non-resonant FWM at 321.0 nm with the time delay. (d) The temporal evolution of the 329.3 nm radiation measured versus the time delay over the 100 ps timescale.

Fig. 3 (a) The 329.3 nm radiation induced by 800 nm and 1910 nm lasers versus the time delay. The spectrum at zero delay is shown in inset. (b) The 330.8 nm radiation induced by 800 nm and 2070 nm lasers versus the time delay. The spectrum around zero delay is shown in inset. (c) The spectrum obtained by injecting the 800 nm laser and a 330 nm seed with the 0.5 ps delay into 80 mbar nitrogen gas. The radiation and absorption peaks ascribed to $B(v=2,3,4) \rightarrow X(v=0,1,2)$ with $\Delta v = 2$ are indicated with black arrows, and the corresponding vibrational states are shown in the brackets. Red dotted line indicates the seed spectrum.

Fig. 4 (a) Intensity of the calculated output 800 nm (E_1) pulse with initial population $\rho_{BB}(0) = 0, 0.1, 0.2, 0.4$. The 1580 nm (E_2) pulse injected at the 1 ps delay is indicated by the orange filled curve. Temporal evolutions of $|\rho_{BA}|$ for the cases of (b) $\tau = 0$ and (c) $\tau = 1$ ps with $\rho_{BB}(0) = 0, 0.1, 0.2, 0.4$.

Fig. 5 Calculated spectra of the signal in the cases of (a) $\tau = 0$ and (b) $\tau = 1$ ps with $\rho_{BB}(0) = 0, 0.1, 0.2, 0.4$. (c) Integral of the signal intensity versus τ for different $\rho_{BB}(0)$.

Figure 1

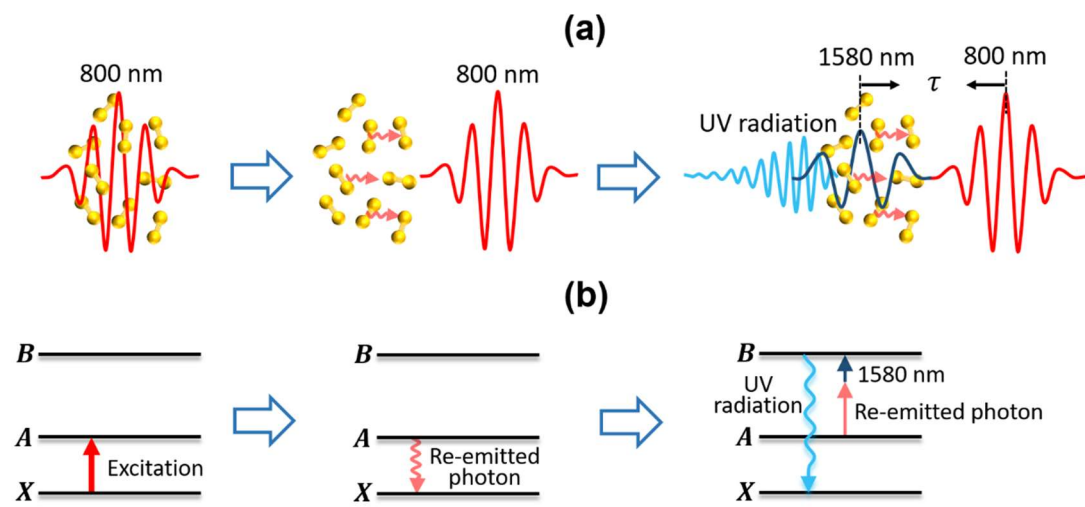


Figure 2

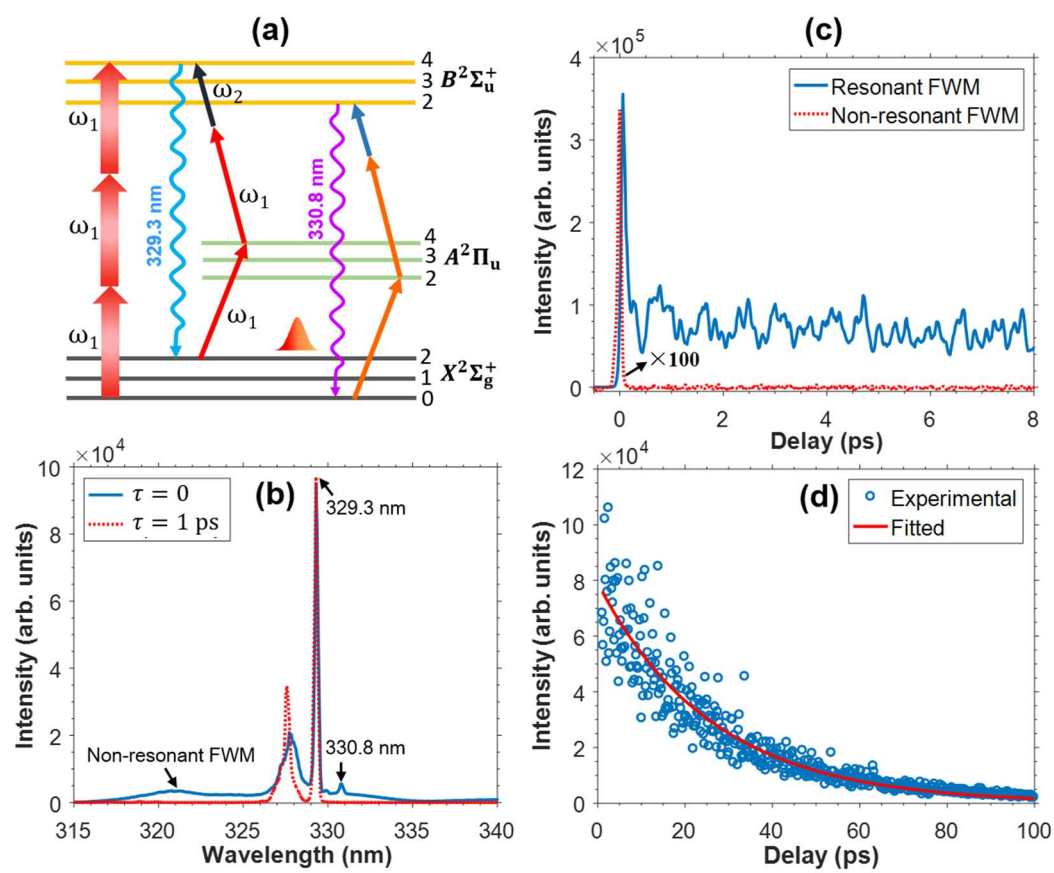


Figure 3

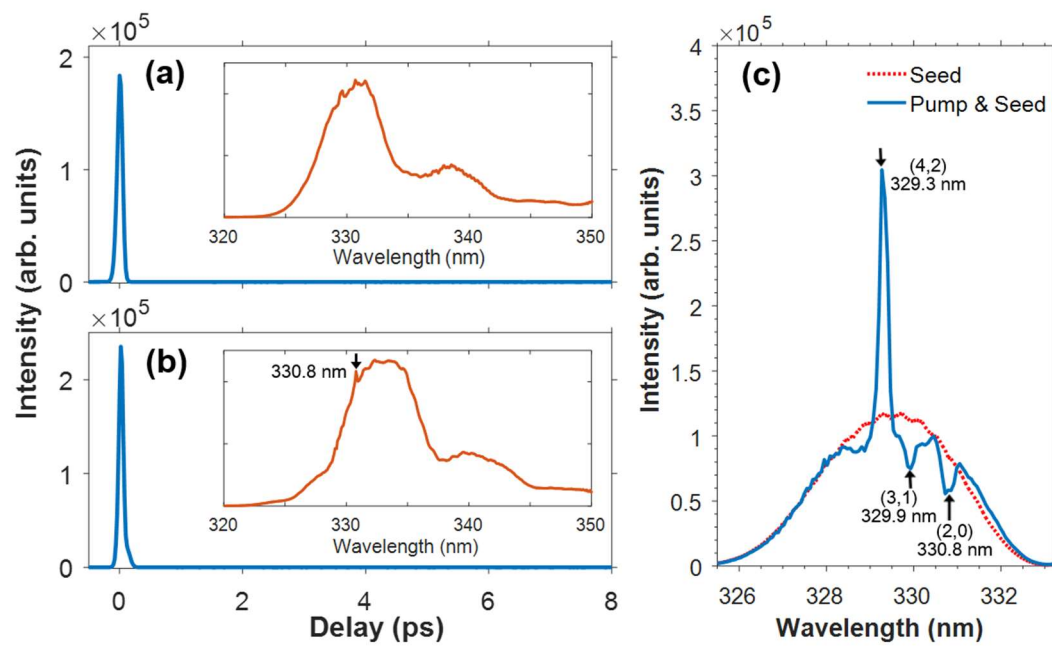


Figure 4

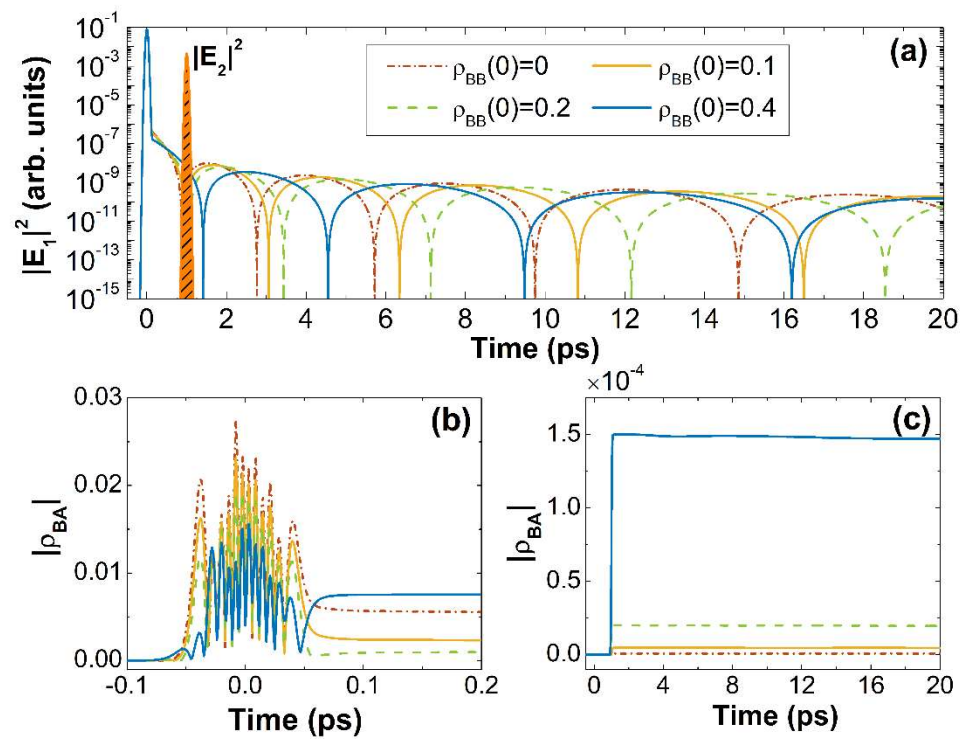


Figure 5

